Decay of ^{142}Ba to levels of odd-odd ^{142}La

C. Chung* and W. B. Walters
Department of Chemistry, University of Maryland, College Park, Maryland 20742

D. S. Brenner and A. Aprahamian
Department of Chemistry, Clark University, Worcester, Massachusetts 01610

R. L. Gill, M. Shmid,† R. E. Chrien, and L.-J. Yuan*
Physics Department, Brookhaven National Laboratory, Upton, New York 11973

A. Wolf‡ and Z. Berant‡
Physics Department, Brookhaven National Laboratory, Upton, New York 11973
and Ames Laboratory, Iowa State University, Ames, Iowa 50010

(Received 28 December 1982)

The γ- and β-ray radiation following the decay of ^{142}Ba to ^{142}La were measured in experiments in which β end-point energies, $\beta\gamma$ coincidences, γ-ray singles, $\gamma\gamma t$ coincidence, and $\gamma\gamma t(\theta)$ angular correlation data were collected. The ^{142}Ba activity was produced by on-line mass separation from the ^{235}U(n_{th},f) reaction. A level scheme for odd-odd ^{142}La was deduced from coincidence information that includes 90 γ rays which are placed among 23 levels. A 0.87 ± 0.17 μs isomeric state was established at 145 keV. The Q_β value of 2200±25 keV was determined from β-γ coincidence data. Beta-ray intensities and logft values have been evaluated, and along with internal conversion and angular correlation measurements, yielded spin-parity assignments for a number of levels. The low-lying levels were compared with level schemes projected from $\pi\nu$ multiplet parabolas computed using parameters extracted from parabolic fits in ^{140}La and ^{142}Pr.

[RADIOACTIVITY ^{142}Ba [from ^{235}U(n_{th},f)] measured E_γ, I_γ, E_β, α_k, $\gamma\gamma t$ coincidence, $\gamma\gamma t(\theta)$ angular correlation, $\beta\gamma$ coincidence; HPGe β and γ detectors; ^{142}LA deduced levels J^π, I_β, δ, logft, level lifetime, and Q_β. Mass separated ^{142}Ba activity.]

I. INTRODUCTION

Extensive consideration has been given to the interactions between protons and neutrons in odd-odd nuclei. "Rules" have been devised to predict the spin or spins of the lowest lying levels in odd-odd nuclei by Nordheim,[1] Gallagher and Moszkowski,[2] and Brennan and Bernstein.[3] The energy dependence of the members of the multiplets formed by the coupling of the proton and neutron has been discussed by deShalit,[4] Sasaki,[5] Schiffer,[6] and Molinari, Johnson, Bethe, and Alberico.[7] Most of the nuclides considered by these authors have been near double magic nuclides such as ^{16}O, ^{40}Ca, ^{90}Zr, and ^{208}Pb. The dominant interaction has been found to be a delta function interaction between the proton and neutron with residual interactions described by dipole and quadrupole interactions.

In a recent letter, Chiang, Wang, and Hsieh[8] calculated the low-lying levels of the odd-odd ^{140}La, ^{142}Pr, and ^{144}Pm nuclides using a modified surface delta interaction between the proton and neutron. Their results were not in good agreement with the experimental data.

Paar[9] and Arvay *et al.*[10] have drawn attention to the parabolic relationship between the energy values for the members of a $\pi\nu$ multiplet and the quantity $I(I+1)$ when the interaction between the proton and neutron is largely of dipole and quadrupole character. Subsequently, we have shown that the odd-odd $N=83$ nuclides can be interpreted almost entirely on the basis of a quadrupole interaction.[11] In this paper we extend the analysis to the levels of the $N=85$ nuclide ^{142}La and compare the projected structure to the results of new experimental studies of the levels of ^{142}La populated in the decay of ^{142}Ba.

II. EXPERIMENTAL MEASUREMENTS

The decay properties of fission product ^{142}Ba, along with the fission process, were first studied by Hahn and Strassmann.[12] Extensive studies of the decay of ^{142}Ba were made almost simultaneously by McIssac and Murri,[13] and Larsen, Talbert, and McConnell,[14] and a level scheme for ^{142}La with 52 γ transitions placed among 21 levels was proposed. Unfortunately, neither of these studies yielded any spin-parity assignment for excited levels. Fritze and Kennett[15] reported a Q_β value for ^{142}Ba decay based on β-γ coincidence measurements using NaI scintillation detectors. The present experiments were designed to refine and extend the existing level scheme of ^{142}La, assign spins and parities to as many levels as possible through angular correlation studies, and to determine β end-point energies and a more precise Q_β value.

 ©1983 The American Physical Society

TABLE I. Energies, intensities, and placements of γ rays from the decay of ^{142}Ba. The parentheses denote the uncertainties in the last digits of the energies and intensities. The absolute γ ray intensity per 100 decay for present work is obtained by multiplying $I_{\gamma(\mathrm{rel})}$ by 0.0211. Here, as elsewhere in this paper, energy values for γ rays and levels are discussed without the decimal point or following digits.

E_γ (keV)	I_γ (rel)	I_{tot}	From—to
8.7[a]		32(3)	309—300
63.6(1)	4.4(6)[b]	23(3)	364—300
68.3(1)	3.8(5)[b]	16(2)	432—364
68.3(1)	4.0(9)[b]	37(8)	145—77
69.7(1)	12.8(6)	54(3)	147—77
77.6(1)[c]	462(16)	1572(51)	77—0
79.8[d]	1.8(6)	5.8(19)	335—255
84.0[d]	1.5(5)	4.5(15)	231—147
123.0(1)	45.0(16)	73(3)	432—309
130.0[d]	3.0(8)	4.5(12)	361—147
147.5[d]	3.6(6)	5(1)	147—0
153.1(1)	4.2(10)	5.6(13)	300—147
154.6(1)	23.6(14)	31(2)	300—45
162.3(1)	5.5(4)	7.1(5)	309—147
172.6(3)	1.8(7)	2.2(9)	604—432
177.0(1)	84(2)	103(3)	432—255
215.7(2)	5(2)	5.9(2)	361—145
216.6(1)	10(2)	11(2)	364—147
220.2(2)	3.2(6)	3.3(6)	1204—981
222.8(1)	15.7(5)	17.6(6)	300—77
231.6(1)[c]	591(12)	656(13)	309—77
242.9(2)	9(2)	10(2)	604—361
253.7(1)	26(2)	29(3)	1458—1204
255.3(1)[c]	1000(23)[e]	1084(25)	255—0
257.5(1)	6.8(16)	7.3(18)	355—77
269.5(1)	45(4)	48(5)	604—335
283.5(2)	14(4)	15(4)	361—77
286.3(1)	54(4)	57(4)	364—77
309.2(1)	126(4)	132(5)	309—0
335.0(1)	71.5(6)	74.4(6)	335—0
337.7(2)	15.1(11)	15.2(11)	1204—866
340.5(7)	1.2(10)	1.2(10)	417—77
346.8(2)	6.5(6)	7.0(6)	425—77
354.7[d]	2.4(8)	2.4(8)	432—77
356.8[d]	4.0(12)	4.1(12)	666—309
364.0(1)[c]	230(7)	238(7)	364—0
379.4(1)	28.1(6)	28.9(6)	1458—1078
380.0[d]	3.2(11)	3.3(11)	984—604
412.7[d]	2.7(13)	2.7(13)	1078—666
417.8(2)	18(2)	18(2)	417—0
425.1(1)[c]	279(5)	285(5)	425—0
432.3(1)	50(4)	51(4)	432—0
434.4(1)	22(3)	22(4)	866—432
448.3(1)	12.1(7)	12.2(7)	1457—1010
457.1(1)	18.2(7)	18.5(7)	604—147
473.4(1)	20.3(7)	20.4(7)	1457—984
488.3(2)	4.5(7)	4.5(7)	1457—969
537.2(2)	3.4(6)	3.4(6)	969—432
557.7(1)	12.0(5)	12.1(5)	866—309
558.4(2)	4.4(7)	4.4(7)	666—77

A. Source production

The relatively long-lived ^{142}Ba ($t_{1/2}=10.6$ min) and its short-lived parent ^{142}Cs ($t_{1/2}=1.8$ s) were produced from fission in an integrated target-ion source assembly in the on-line mass separator TRISTAN. The operation of the TRISTAN facility and the associated data acquisition system has been described in detail by Gill *et al.*[16] and references therein. For these experiments, the facility employed a high-temperature surface-ionization source described by Shmid, Gill, and Chung,[17] that contained a graphite cloth impregnated by 5 g of 93% enriched ^{235}U. The power input to the ion source for these experiments was up to 1600 W, corresponding to a maximum target

TABLE I. (*Continued.*)

E_γ (keV)	I_γ (rel)	I_{tot}	From—to
577.7(2)	3.3(5)	3.3(5)	1010—432
590.7(1)	15.1(7)	15.1(7)	1457—866
599.8(1)	89.8(10)	90(1)	1204—604
604.3(2)	20.4(10)	21(1)	604—0
620.3(3)	2.4(6)	2.4(6)	984—364
622.8(2)	3.2(6)	3.2(6)	984—361
649.3(2)	3.4(6)	3.4(6)	984—335
654.6(2)	4.3(6)	4.3(6)	1078—425
660.9(1)	11.0(6)	11.1(6)	1078—417
674.4(6)	3.2(13)	3.2(13)	984—309
674.7(7)	3.4(13)	3.4(13)	1010—335
714.4(4)	2.0(7)	2.0(7)	969—255
769.4(1)	36.7(9)	36.7(9)	1079—309
771.9(2)	4.6(7)	4.6(7)	1204—432
786.6(2)	9.2(7)	9.2(7)	1204—417
791.6(2)	4.1(7)	4.1(7)	1457—666
823.4(3)	14(5)	14(5)	1078—255
840.4(1)	176(6)	177(6)	1204—364
853[d]	1.5(8)	1.5(8)	1457—604
895.2(1)	676(19)	677(19)	1204—309
907.2(4)	2.0(7)	2.0(7)	984—77
931.6(4)	4(3)	4(3)	1078—147
932.6(9)	4(3)	4(3)	1010—77
934[d]	1.5(8)	1.5(8)	1539—604
949.1(1)	517(13)	518(13)	1204—255
984.5(3)	3.6(7)	3.6(7)	984—0
1001.2(1)	474(12)	474(12)	1078—77
1033.0(1)	16.7(7)	16.7(7)	1457—425
1040[d]	3.8(13)	3.8(13)	1457—417
1078.7(1)	559(16)	559(16)	1078—0
1094.1(1)	137(6)	137(6)	1457—364
1114.4(4)	5(2)	5(2)	1539—425
1122.9(1)	19.1(8)	19.1(8)	1457—335
1126.8(1)	73(6)	73(6)	1204—77
1148.7(1)	24.3(9)	24.3(9)	1457—309
1202.4(1)	270(10)	270(10)	1457—255
1204.3(1)	694(11)	694(11)	1204—0
1230.2(2)	4.1(4)	4.1(4)	1539—309
1283.6(3)	3.2(6)	3.2(6)	1539—255
1380.2(1)	166(8)	166(8)	1457—77

[a]The 8.7 keV γ ray was not observed. Here the I_{tot} was deduced from the coincidence spectra.
[b]γ-ray intensities were also deduced from coincidence spectra.
[c]The values measured for these γ rays by Borner *et al.* (Ref. 21) using a curved crystal spectrometer are 77.6(1), 231.52(4), 255.12(4), 363.80(5), and 425.03(6).
[d]γ-ray energies and intensities were deduced from coincidence spectra with uncertainty values >0.4 keV.
[e]Fiducial γ ray whose intensity is set equal to 1000.

temperature of about 1930 °C.

The target-ion source system was irradiated in an external neutron beam with a flux of

$$1.5\times10^{10}\ \text{ncm}^{-2}\ \text{s}^{-1}$$

from the 40 MW_{th} high flux beam reactor at Brookhaven National Laboratory. The $A=142$ ion beam was deposited onto an aluminized mylar tape in a moving tape collector. Maximum saturation activity at the deposit point was estimated by β and γ counting to be 175 μCi. In order to suppress the ^{142}Cs parent and reduce the large activity of ^{142}Ba, experiments were performed either at the deposit point (parent port) with low input power ($\sim$1000 W) or at a secondary station 60 cm downstream (daughter port) with various time sequences to transport the activity from the parent port to the daughter port.

B. Experimental measurements

Seven Ge detectors were employed in these studies. For the $\gamma\gamma t(\theta)$ studies, four cylindrical detectors with active volumes of 76, 78, 79, and 92 cm^3, all having a system full width at half maximum (FWHM) of ≤ 1.8 keV at 1.33 MeV were used. The low-energy γ rays were measured

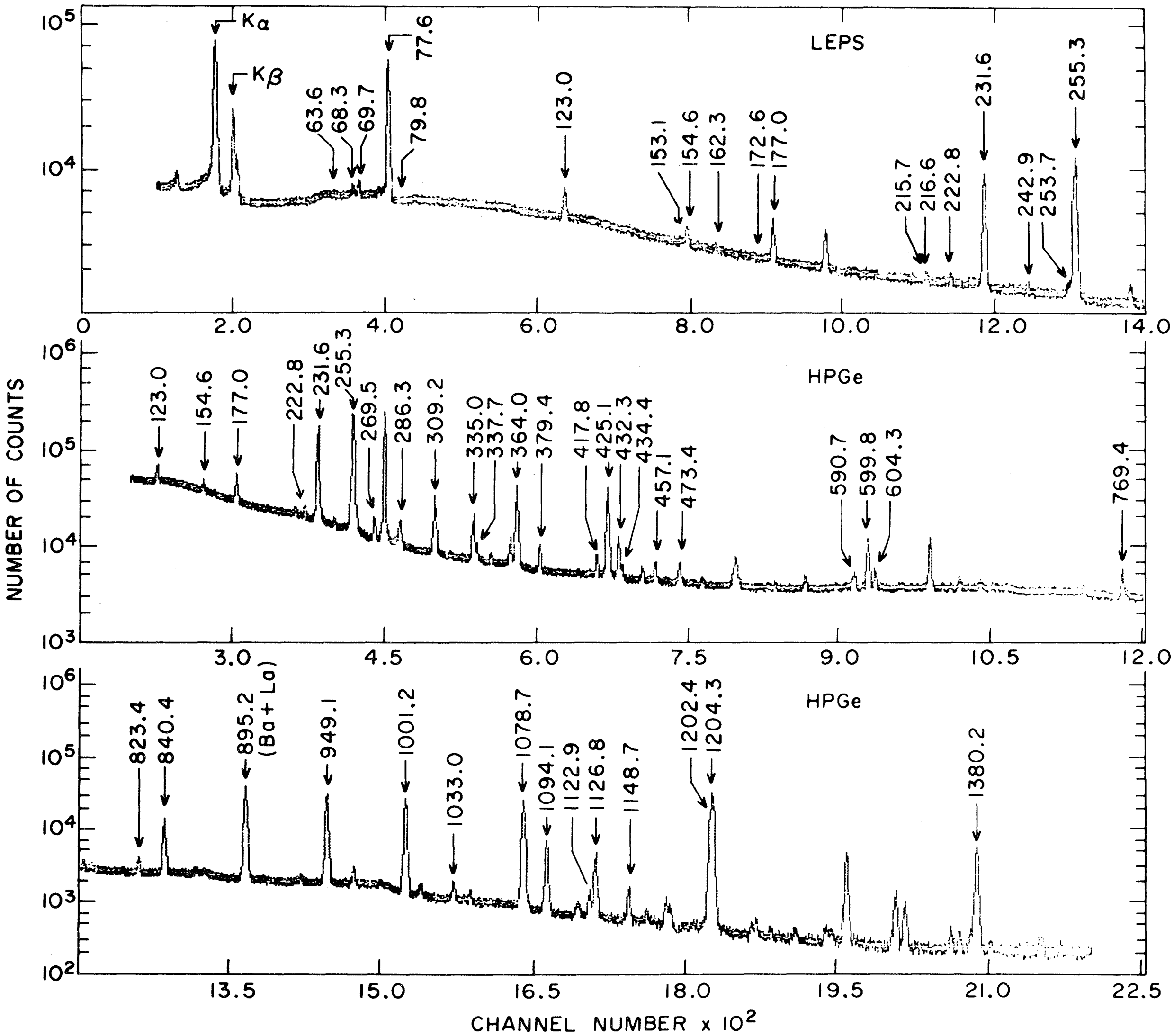

FIG. 1. Singles spectra of ^{142}Ba decay. The top spectrum ($E_\gamma < 260$ keV) is excerpted from the measurements taken with the 2-cm^3 planar Ge detector. The lower sections are part of a spectrum taken with a large high purity (HP) Ge detector. Only γ rays belonging to ^{142}Ba decay with $I_\gamma > 15$ are labeled.

with 2-cm^3 and 5-cm^3 low energy photon spectrometer (LEPS) planar detectors with FWHM of 545 eV at 122 keV, and a Ge detector (250 mm^2 surface area, 10 mm active thickness) mounted in a cryostat equipped with a 12-μm Ti entrance window was used to measure β spectra. The detector arrangement and activity enhancement for each measurement are discussed below.

1. $\gamma\gamma$ coincidence and angular correlation measurements

For the coincidence and angular correlation studies, the four detectors were each positioned 7.5 cm from the activity at the daughter port. One of the detectors, an n-type Ge detector with an energy threshold of 20 keV, was used to measure the K x rays for internal conversion measurements. To suppress both the 1.8-s ^{142}Cs parent and the 92.5-min ^{142}La daughter activities, the $A=142$ ion beam was collected at the parent port for 600 s, delayed for 20 s before it was moved to the daughter port where the four detectors are located, and counted for 600 s.

The development and testing of the four-detector system has been described earlier.[18] The four detectors were arranged in an angular correlation apparatus and cross talk was reduced with sheets of Cu and Pb shielding. This array provided data at 90°, 105°, 120°, 135°, 150°, and 165°. Each coincidence event that was written on tape included two $8K$ digitized γ-ray energy signals and their respective detector identification bits, as well as digitized time-to-amplitude converter (TAC) signal. The TAC signal was derived from a priority routing circuit that directs the first of any pair of timing signals to the TAC start input and the second to the TAC stop input. The data were normalized by using $2K$ signals spectra from each detector col-

TABLE II. Coincidence relationships of some γ transitions in ^{142}La levels. Qualitative indication of coincidence: S=strong, M=moderate, W=weak, D=delayed.

Coincidence with E_γ (keV)	Energy window E_γ (keV) 77	255	379	448	473	599	Coincidence with E_γ (keV)	Energy window E_γ (keV) 77	255	379	448	473	599
68	*M*						557	*M*					
69	*S*					*M*	577				*W*		
77			*M*	*M*	*M*	*M*	588	*W*					
123	*S*						590	*M*	*M*				
153	*M*					*W*	599	*M*	*W*				
154	*D*			*W*	*W*	*W*	604						*M*
162	*M*						620					*W*	
172						*W*	622					*W*	
177		*S*					649					*W*	
215	*W*						654			*W*			
216	*M*						660	*M*		*W*			
222	*M*						674.4					*W*	
231	*S*	*W*	*M*		*M*		674.7				*W*		
242	*M*					*M*	714		*W*				
253		*M*				*W*	769	*M*					
255			*M*	*W*	*W*	*W*	786	*W*					
269	*M*					*S*	823		*M*				
283	*M*				*W*		840	*M*					
286	*S*						853						*W*
309					*W*		895	*S*					
335				*W*	*W*	*M*	907					*W*	
337	*M*						931	*M*		*W*	*W*		
340	*W*						934						*W*
346	*M*						949		*S*				
354	*W*						984					*W*	
364					*W*		1001	*S*		*M*			
379	*M*	*M*					1078			*M*			
412	*W*		*W*				1094	*M*					
425			*M*				1126	*M*					
434		*W*					1148	*W*					
448	*M*						1202		*S*				
457	*M*					*M*	1230	*W*					
473	*M*						1283		*W*				
488	*M*	*W*	*W*				1380	*M*					
537		*W*											

lected simultaneously at the same dead time rate with a single ADC and a four-channel multiplex mixer. These singles spectra were gated by the constant fraction discriminator on each channel to reflect the actual coincidence efficiency. Approximately 4×10^7 $\gamma\gamma(\theta)t$ events of ^{142}Ba data were collected in these experiments.

2. *Singles measurements*

Singles spectra were taken at the daughter port using the LEPS and the n-type Ge detector at various source-to-detector distances (from 3 cm to 22 cm) to identify sum peaks and summing contributions to crossover γ rays. To further suppress the ^{142}Cs parent and ^{142}La daughter activities, sources were collected at the parent port at low input power for 300 s, allowed to decay for 30 s, then moved to the daughter port where activity was measured for 300 s. Gamma-ray energies and intensities free from summing contributions were derived from these singles spectra.

3. *Beta-ray end-point energy measurements*

Beta-ray end-point energies for ^{142}Ba decay were measured using the Ge β detector and a Ge γ detector in a coincidence arrangement. The β detector cryostat was integrally mounted into the vacuum system of the moving tape collector so that the source-to-detector distance was $\sim$15 mm. The γ detector was located approximately the same distance from the source at an angle of 180° with respect to the β detector.

The γ-ray sensitivity of the β detector was employed as a means for energy calibration using high energy neutron capture γ rays and the many well known γ rays of ^{90}Rb measured on-line at the separator.[19] Determination of energy loss for β rays in the 12 μm Ti entrance window and detector dead layer was made using a ^{210}Bi conversion electron source. To minimize systematic errors in β-spectrum end-point determinations due to accidental summing, pulse pileup rejection circuitry was used and counting rates were kept below 3 kHz. Two-point pulser stabilization of the analog-to-digital converter was used to com-

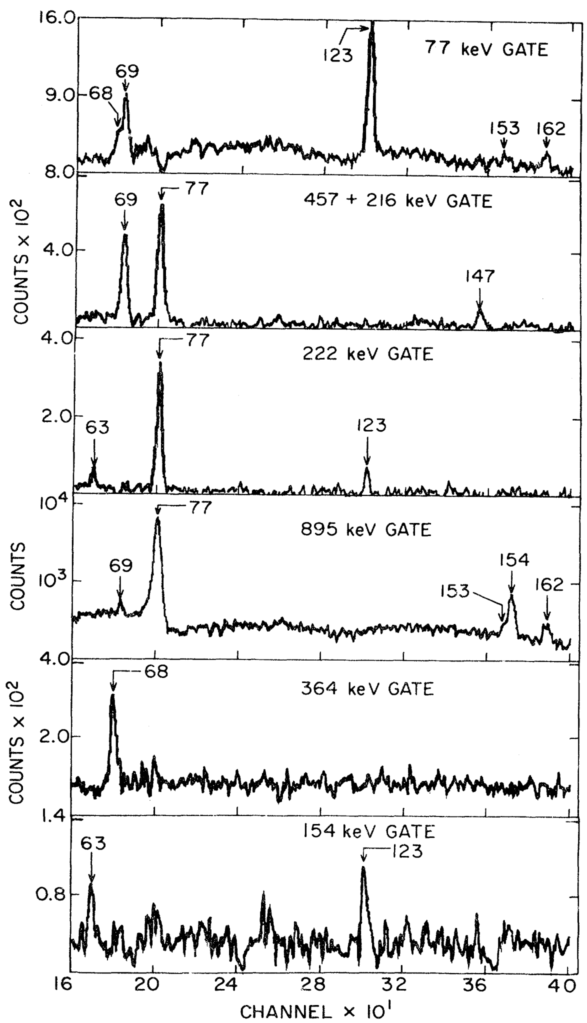

FIG. 2. Selected $\gamma\gamma$ coincidence spectra supporting the placement of the 64-, 68-, 69-, 147-, 153-, and 154-keV γ rays.

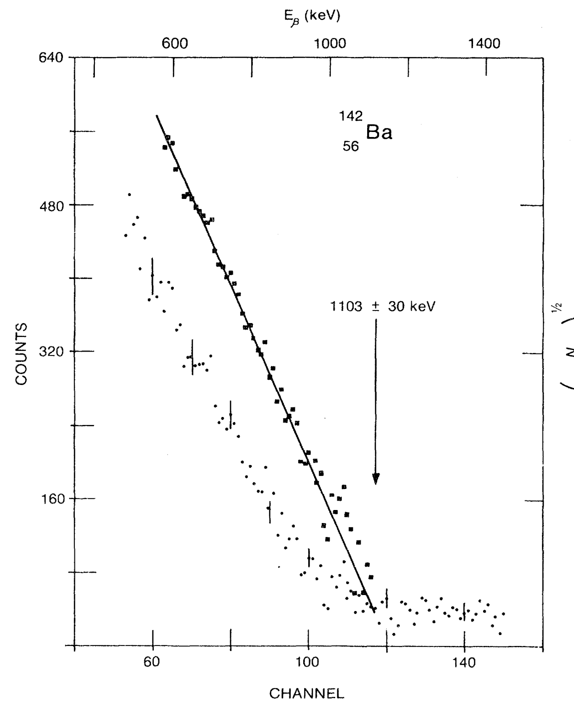

FIG. 3. The β spectrum in coincidence with the 1001- and 1078-keV γ-ray gates in ^{142}Ba decay. The Fermi-Kurie fit to the data is also shown.

pensate for the long-term electronic drift during the experiment.

The β-γ coincidence data, recorded in event mode on magnetic tape, were sorted off-line into spectra for various β branches. Fermi-Kurie analysis of β spectra was performed using an interactive computer code BDK developed by Rehfield.[20] This procedure was used to linearize data in the high energy region of the β spectrum, as shown in Fig. 3, permitting a precise determination of the end point.

III. RESULTS

A. Energy and intensity values for the γ transitions

Gamma rays observed in the singles spectra have been assigned to ^{142}Ba decay by their half-lives and by their appearance in coincidence spectra gated on strong transitions. Sum peaks and summing contributions to crossover γ rays have been removed by comparing intensity differences among spectra measured at different source-to-detector distances. By these procedures, assignment to ^{142}Ba decay, ^{142}La decay, or background was made for all but a few γ rays observed in the singles spectra. The energy value, relative intensity, total transition intensity, and placement in the level scheme for each γ ray shown in Fig. 4 are listed in Table I. Several close-lying doublets reported earlier[13,14] have been resolved in the high resolution LEPS spectra. Selected segments of the singles spectra taken from the LEPS and n-type Ge detectors are illustrated in Fig. 1.

B. Coincidence data

A total of 39 gated spectra were generated by scanning the event mode data. Each gate was set for all six angles at both directions among the four detectors. From these results a level scheme for ^{142}La has been deduced which contains a total of 23 excited levels with 90 γ rays placed among them. The positions of 39 γ transitions proposed earlier[13,14] are confirmed while γ transitions out of previously reported levels at 155, 591, 792, 818, and 1283 keV have been relocated to others including newly assigned levels at 145, 417, 666, 969, 984, 1010, and 1539 keV. Results of additional selected gates are summarized in a qualitative manner in Table II. In Fig. 2 are shown the low-energy portions of several gates that contain evidence for the placement of the doublet 68-keV transitions and the 8.7-keV transition as well as the placement of the 145- and 147-keV levels.

C. Angular correlation data

Integrated peak areas of the strong coincidences for each angle in both detectors were normalized by the

TABLE III. Gamma-gamma angular correlation results for γ rays in ^{142}La. The δ values are derived from the A_2 (only) data using the tables of Taylor *et al.* (Ref. 23).

Cascade	c/angle	A_2	A_4	A_2 (only)	Sequence	δ	δ_2
840-364	4500	0.15(3)	0.00(4)	0.15(3)	$1^+(E1)\underline{2}^-(E2/M1)2^-$	−0.74(15)	−4.6(25)
1094-364	2600	0.17(4)	0.03(5)	0.17(3)	$\underline{1}^+(E1)2^-(E2/M1)2^-$	−0.83(21)	−3.6(17)
840-286	1300	−0.15(4)	0.08(6)	−0.15(4)	$1^+(E1)2^-(E2/M1)1^-$	−0.42(7)	>12(6)
					$1^+(E1)2^-(E2/M1)2^-$	−0.05(8)	+2.6(7)
1094-286	800	−0.22(5)	0.09(7)	−0.22(5)	$1^+(E1)2^-(E2/M1)1^-$	0.54(11)	+7.7(92)
					$1^+(E1)2^-(E2/M1)2^-$	0.09(10)	+1.8(5)
949-255	22 000	0.05(3)	0.01(4)	0.05(3)	$1^+(E1)1^-(E2/M1)2^-$	−0.26(16)	1.7(5)
177-255	16 000	0.03(3)	0.01(4)	0.03(3)	$0^-(M1)1^-(E2/M1)2^-$	−0.03(5)	−3.0(5)
895-309	4000	0.13(4)	0.09(5)	0.15(3)	$1^+(E1)\underline{2}^-(E2/M1)2^-$	−0.74(15)	4.6(25)
895-231	23 000	−0.10(2)	0.02(4)	−0.09(2)	$1^+(E1)2^-(E2/M1)1^-$	0.33(3)	−23(29)
					$1^+(E1)2^-(E2/M1)2^-$	−0.16(4)	3.7(7)
1033-425	300	−0.14(6)	−0.04(10)	−0.13(6)	$1^+(E1)1^-(E2/M1)2^-$	0.31(24)	>5(10)
600-269	2200	0.27(4)	0.02(5)	0.28(4)	$1^+(E1)1^-(E2/M1)1^-$	0.22(6)	4.6(18)
					$1^+(E1)2^-(E2/M1)1^-$	−0.14(7)	−1.8(3)
600-604	550	0.06(10)	0.01(15)	0.06(10)	$1^+(E1)1^-(E2/M1)2^-$	−0.30(34)	+1.5(25)
					$1^+(E1)2^-(E2/M1)2^-$	0.44(10)	∞
600-457	600	0.06(5)	0.05(7)	0.08(6)	$1^+(E1)1^-(E2/M1)1^-$	−0.06(8)	−17(33)
					$1^+(E1)1^-(E2/M1)2^-$	−0.42(28)	−1.2(10)
					$1^+(E1)2^-(E2/M1)1^-$	0.12(8)	−3.9(17)
					$1^+(E1)2^-(E2/M1)2^-$	−0.5(2)	< −10
557-231	700	0.01(13)	0.03(20)				
123-309	1600	0.03(4)	−0.02(7)				
269-335	3500	0.02(3)	−0.02(5)				
434-123	300	0.034(14)	0.22(23)				
434-177	350	0.088(63)	0.08(10)				

respective peaks in the singles spectra. The results were least-square fitted to the angular distribution function

$$W(\theta)=1+A_2P_2(\cos\theta)+A_4P_4(\cos\theta) .$$

The data were also fitted to the function

$$W(\theta)=1+A_2P_2(\cos\theta)$$

for those cascades in which an $E1$ γ ray from the 0^+ or 1^+ levels fed into low-lying negative parity levels. The uncertainties of A_2 and A_4 were determined by standard statistical methods. Correction for the finite solid angle of the Ge detectors was derived from the tables of Camp and Van Lehn[22]; correction for the dead time loss in the priority box was made by comparing the record rates for each detector as described in Wolf *et al.*[18] Results of corrected values of A_2 and A_4 for some strong cascades, as well as possible spin-sequences and mixing ratios, are listed in Table III. The conventions adopted are from those of Becker and Steffen.[24]

D. Internal conversion results

The α_k values for transitions at 63, 68, 69, 77, 123, 231, and 255 keV were deduced from the coincidence spectra taken with the detector with the 20-keV threshold. The α_k values were computed from the ratio of x rays to γ rays in gates in which the transition of interest is the only low energy γ ray present or is present only with γ rays whose α_k values are known. Although the uncertainties from these measurements are large, $E1$ transitions could be distinguished from $M1/E2$ transitions. The resulting α_k values are listed in Table IV.

E. Beta end-point energies

In Fig. 3 we show experimental data and a Fermi-Kurie fit to the end-point region of the ^{142}Ba β spectrum in coincidence with summed 1001- and 1078-keV γ-ray gates in ^{142}La. An end-point energy of 1103±30 keV was determined for this spectrum using the program BDK. Table V contains results for ^{142}La γ-gated β spectra. The data yield a mean Q_β value of 2200±25 keV for the ^{142}Ba-^{142}La doublet mass difference. This result is in excellent agreement with the value reported by Fritze and Kennett,[15] 2200±100 keV.

F. Level half-life

The half-life of the 145-keV level was measured by gating a time-to-amplitude converter (TAC) with stop signals from a single channel analyzer set on the 154-keV peak in the 78 cm^3 n-type Ge detector spectrum and start signals from a single channel analyzer set on the 63- to 77-keV peak region in the 5-cm^3 LEPS spectrum. Random and Compton background events were measured with a second experiment with stop signals from the 231-keV peak and start signals from the 63- to 77-keV peak region. A value of 0.87±0.17 μs was determined.

IV. CONSTRUCTION OF THE DECAY SCHEME OF ^{142}Ba

The level scheme from the decay of ^{142}Ba is shown in Fig. 4. As can be seen in the decay scheme, every level is supported by at least three populating or depopulating transitions with the exceptions described below.

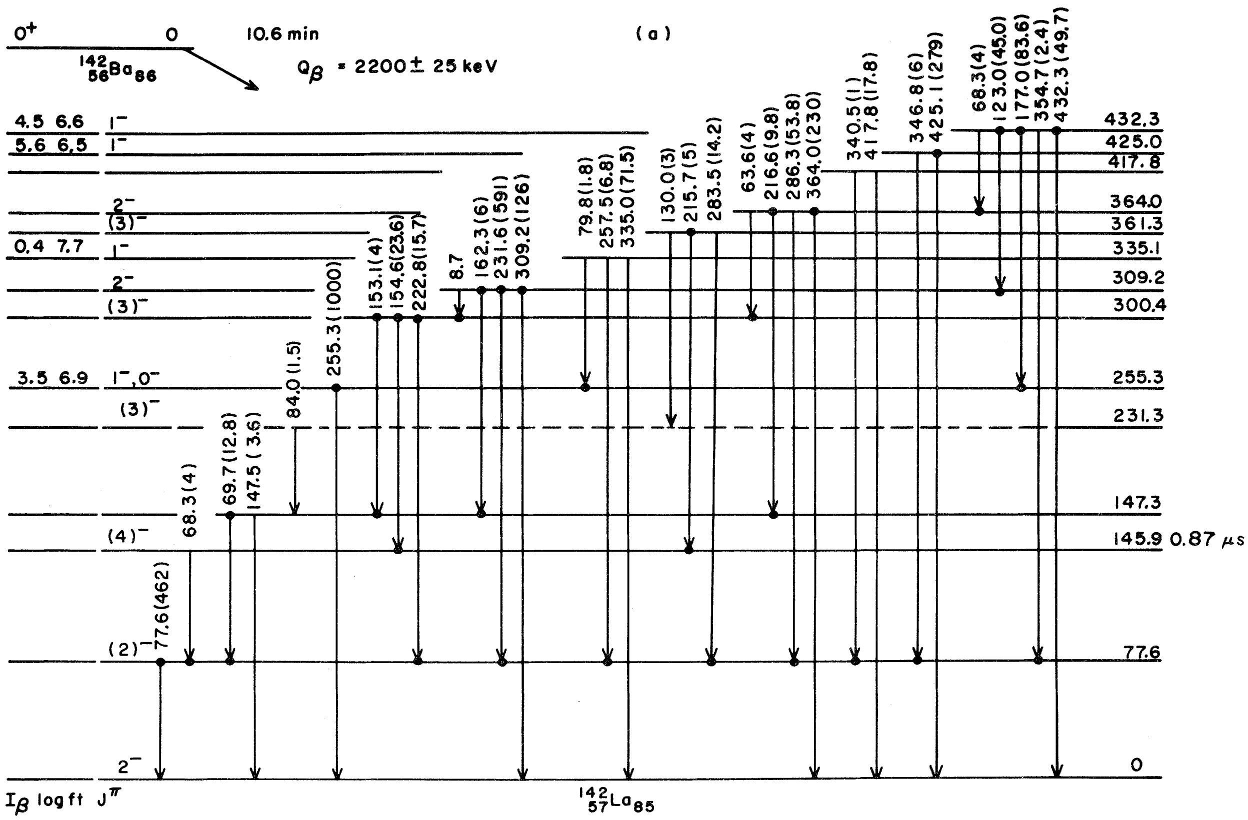

FIG. 4. The decay scheme of 10.6-min ^{142}Ba to levels of the odd-odd nuclide, ^{142}La.

The level at 145 keV has been suggested on the basis of the appearance of an asymmetric broad peak at 68–69 keV in the 77-keV gate as shown in Fig. 2. This peak can be decomposed into 68.3- and 69.7-keV components. The 364-keV gate shows a single symmetric peak of normal width at 68.3 keV and no comparable intensity is observed in the 77-keV peak. The strong coincidences between the 77- and 222-keV γ rays establish a level at 300 keV.

The appearance of the 153-, 154-, 162-, 222-, 231-, and 309-keV γ rays in the 895-keV gate and not in the 1204-keV gate requires that all of these γ rays be placed below 309 keV in the decay scheme. Because the 222-keV γ ray decays from the 300-keV level and shows the 123-keV γ ray in its gate, an 8.7-keV transition between the 309- and 300-keV levels must be postulated. The coincidence between the 153- and 69-keV γ rays easily permits the placement of the 153-keV γ ray. The 154-keV γ ray could either come from the 309-keV level to a level at 154 keV as shown by Larsen *et al.*[14] or from the 300-keV level to the level at 145 keV suggested by the coincidences between the 68- and 77-keV peaks. No prompt coincidences between the 154-keV peak and peaks at 68, 77, or 154 keV are observed either in our studies or those of Larsen *et al.*[14] As the 63-keV peak is observed in both the 154- and 222-keV gates, we postulate that the 154-keV peak must deexcite the 300-keV level to the level at 145 keV. The measurement of the long lifetime of the 145-keV level by observing 154- by 68- and 77-keV delayed coincidences supports this placement.

The total intensity feeding into the 145-keV level from the 154- and 215-keV γ rays is 37±2 intensity units. The intensity of the 68.3-keV γ ray depopulating the 145-keV level is 4.0±0.9 units. The α_T values for 68-keV $M1$ and $E2$ transitions are 3.77 and 8.15, respectively.[25] Only pure $E2$ multipolarity for the 68.3-keV transition can carry out the 37 intensity units that feed into the 145-keV level.

A level at either 231 or 277 keV is suggested by the presence of 84- and 130-keV γ rays in the 242-keV gate. We can find no evidence for any other γ rays feeding into or out of a 277-keV level. Since the γ rays that would deexcite a 231-keV level to the ground or 77-keV levels would be doublets with existing 231- and 154-keV γ rays, respectively, we cannot be certain that these γ rays are not present. As we have less reason to doubt the presence of a level at 231 keV, we have shown a level at that position.

V. BETA-RAY INTENSITIES AND SPIN-PARITY ASSIGNMENTS

A. Ground-state properties and absolute γ-ray intensity

Prestwich and Kennett[26] studied the decay of 92.5 min ^{142}La and β branching to various ^{142}Ce levels and proposed the ground-state spin parity of ^{142}La to be 2^-. The data from a similar study by Larsen, Talbert, and McConnell[14] also supported this assignment. According to the rules of Raman and Gove,[27] the ground-state to ground-

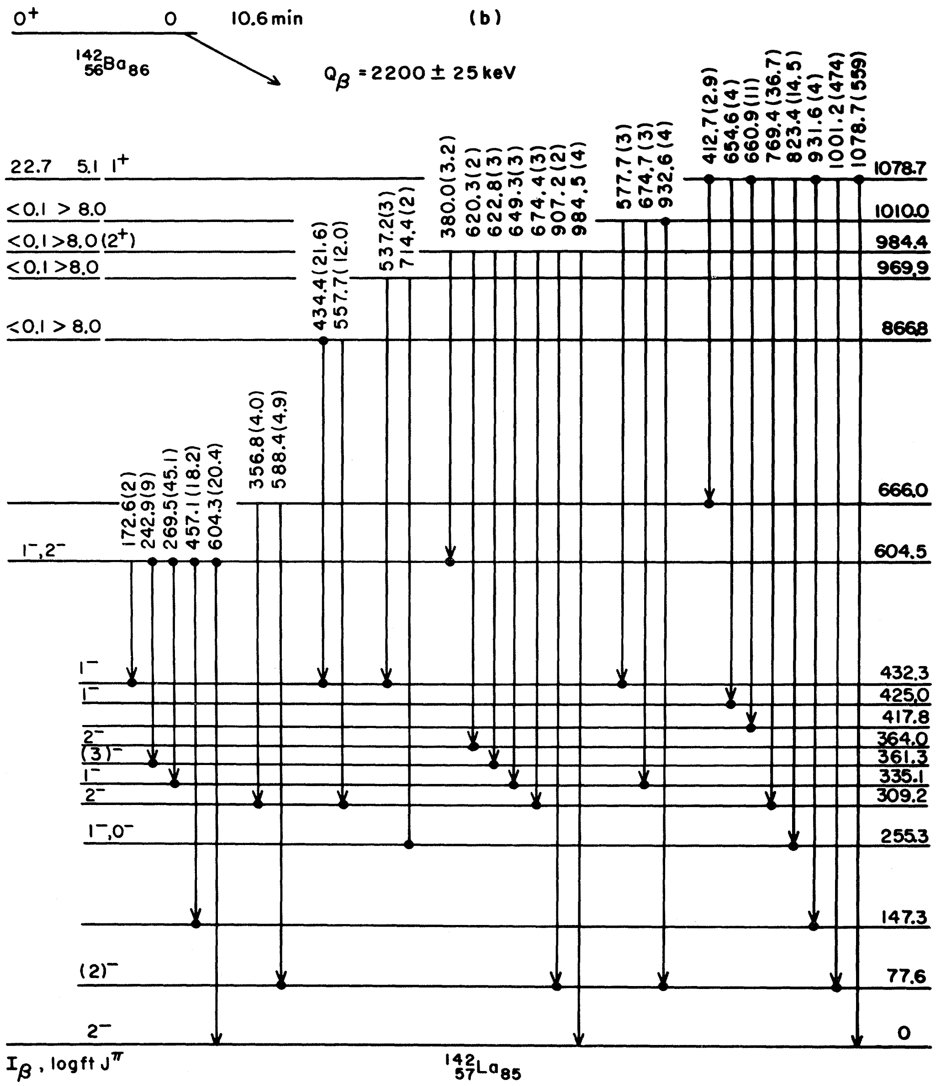

FIG. 4. (*Continued.*)

state β feeding from 0^+ ^{142}Ba to 2^- ^{142}La would be a first forbidden unique transition with $\log f_1 t > 8.5$. With ground-state end-point energy $= Q_\beta$ (2.2 MeV), this would indicate a β branching of $<0.13\%$. Based upon the assumption of little or no ground-state β feeding and the multipolarity assumptions described later, we are able to compute the absolute intensity in ^{142}Ba decay of the 255-keV γ ray to be 0.211 ± 0.006 gamma/decay. This is in good agreement with a recent result of 0.22 ± 0.02, obtained by measuring $A = 142$ saturation activity at the mass separator HELIOS.[28]

B. β-ray branching and log*ft* value for each level

The β-ray branching to a level was calculated from the difference between total transition intensity depopulating and populating that level. The log*ft* value for each level was then computed on the basis of this β-ray intensity value and the experimental Q_β value.

Since substantial transition intensity exists in the form of conversion electrons for low energy γ rays, some assumptions about the multipolarity of the low-energy γ rays must be made in order to compute the total transition intensities. As can be noted in Table IV the α_k values for $M1$ and $E2$ transitions are fairly close to each other and ~ 5 times larger than for $E1$ transitions in the region below 200 keV where conversion coefficients play an important role in the transition intensity. From systematic evidence, we have assumed that all of the levels below 610 keV are negative parity levels and that all of the γ rays depopulating these levels are pure $M1$ except for the 68-keV $E2$ transition out of the 145-keV level. $E1$ multipolarity was assumed for the γ rays depopulating the strongly β-fed levels above 1050 keV to levels below 604 keV.

In order to estimate the possibility of substantial β decay passing through unobserved levels, we have examined the gate on the 255-keV level in detail above the highest

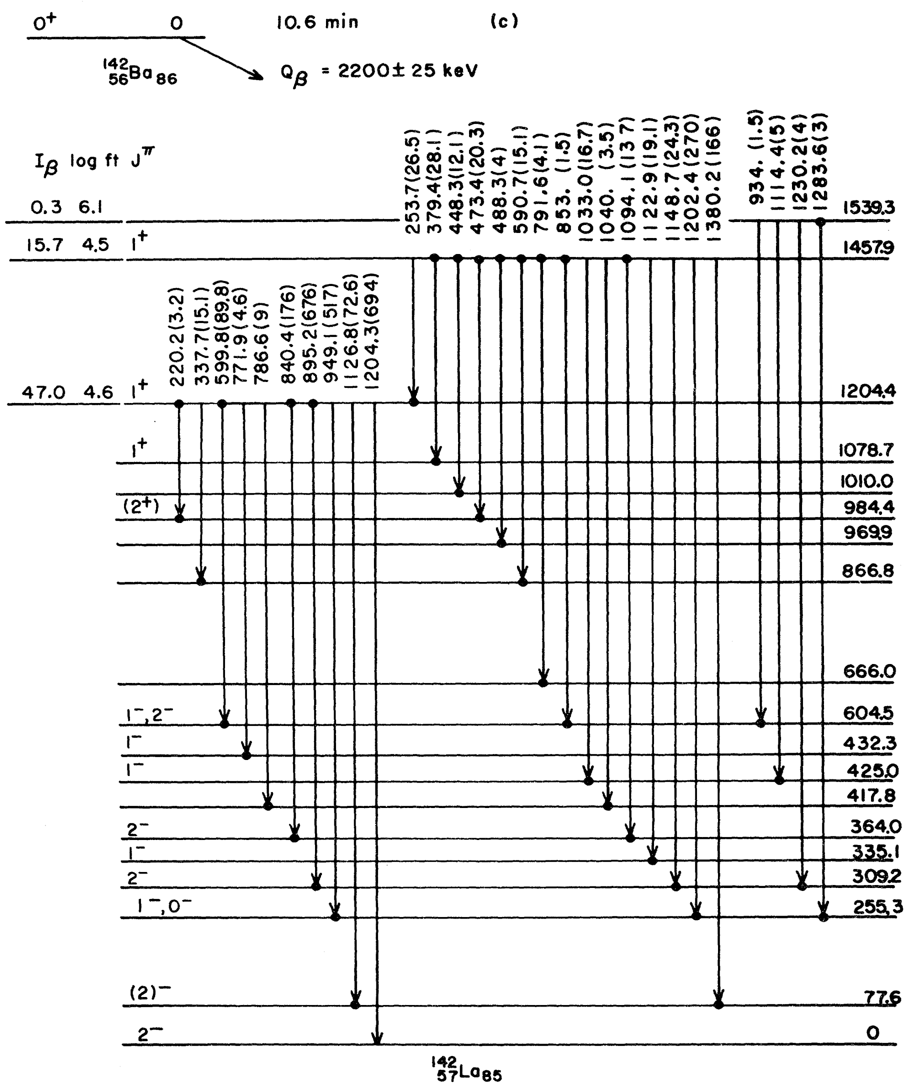

FIG. 4. (*Continued.*)

observed coincident γ ray at 1283 keV. The total counts from 1283 to 1950 keV corrected for detector efficiency and response amounts to only 9 units of γ intensity. A similar comparison was made for the 425-keV γ ray showing little or no net counts. A large number of levels with log*ft* values below 5.0 would be required above 1700 keV to carry significant unobserved β intensity. Total transition intensity is therefore calculated from γ intensity and $M1$, $E1$, or $E2$ conversion coefficients. Since our angular correlation data show both a low and a high δ value for many transitions below 500 keV, small β branches to low-lying levels could be either raised or lowered by $E2$ admixtures, depending on whether the admixed γ ray populates or depopulates a particular level. For that reason, we do not show any β branches $<0.3\%$ to levels below 800 keV.

The three strongest β-fed levels at 1457, 1204, and 1078 keV, receive 85% of the β feeding and have calculated log*ft* values ranging from 4.5 to 5.1, indicating spin and parity of 0^+ or 1^+. Three other levels at 432, 425, and 255 keV, share much of the rest of the β strength and have log*ft* values ranging from 6.5 to 6.8, indicating first forbidden nonunique transitions and restricting their spin parity to 0^- or 1^-. The remaining levels have at most a small percentage of the β feeding consistent with but not requiring spin values >1.

C. Spin and parity assignments for levels in ^{142}La

The spin and parity assignments for a number of levels in ^{142}La have been deduced from the angular correlation results, conversion coefficient data, and β-ray and γ-ray branching.

The three high-lying levels with log*ft* values ≤ 5.1 are taken as positive parity levels. The levels at 1078 and 1204 keV feed the 2^- ground state and must thus be 1^+ states. The 1457-keV level does not feed the 2^- ground state and could be 0^+ or 1^+. The 0^+ possibility is eliminated by the feeding and angular correlations involving the 364-keV level. The A_2 value of 0.15(2) for the 840-364 cascade from the 1^+ level at 1204 through the 364-keV level to the 2^- ground state must be a $1^+(E1)\underline{2}^-(M1/E2)2^-$ cascade as the nonzero A_2 excludes the 0^- choice

TABLE IV. Results of internal conversion coefficient for transition in the decay of ^{142}Ba to ^{142}La.

γ-ray transition E_γ (keV)	Measured α_k value	Theoretical α_k value[a]	Multipolarity assignment
63.6	3.8 ±0.9	$M1=$ 3.52	$M1(E2)$
		$E1=$ 0.69	
		$M2=$46.3	
		$E2=$ 4.12	
68.3[b]	3.3 ±0.5	$M1=$ 2.84	$M1(E2)$
		$E1=$ 0.57	
		$M2=$35.2	
		$E2=$ 3.47	
69.7	2.7 ±0.4	$M1=$ 2.72	$M1(E2)$
		$E1=$ 0.55	
		$M2=$33.4	
		$E2=$ 3.34	
77.6	1.8 ±0.2	$M1=$ 2.05	$M1(E2)$
	2.0 ±0.4[c]	$E1=$ 0.42	
		$M2=$23.4	
		$E2=$ 2.57	
123.0	0.65±0.10	$M1=$ 0.54	$M1(E2)$
		$E1=$ 0.12	
		$M2=$ 4.20	
		$E2=$ 0.66	
231.6	0.09±0.02	$M1=$ 0.098	$M1(E2)$
		$E1=$ 0.022	
		$M2=$ 0.493	
		$E2=$ 0.093	
255.3	0.11±0.02	$M1=$ 0.083	$M1(E2)$
		$E1=$ 0.018	
		$M2=$ 0.403	
		$E2=$ 0.076	

[a]Interpolated from Ref. 25.
[b]Transition between 432 and 364 keV levels.
[c]Data from Ref. 13.

and the $A_2 > +0.10$ excludes the possibility of 1^-. The feeding of this level and the similar A_2 value for the 1094-364 cascade confirm 1^+ spin and parity for the 1457-keV level.

The A_2 value of 0.15(3) observed for the 895-309 cascade from the 1^+ 1204 keV level through the 309 keV excludes the $1^+(E1)1^-(M1/E2)2^-$ cascade and fixes the spin and parity of the 309-keV level as 2^-. The feeding of this level from the 1539-keV level excludes the 0^+ possibility for the spin and parity of that level.

The large positive A_2 value of 0.28(4) for the 600-269 cascade from the 1^+ level at 1204 keV through the level at 604 keV to the level of 335 keV excludes the 0^- possibility for the 604-keV level and both the $1^+(E1)1^-(E2/M1)2^-$ cascade with a maximum A_2 of 0.1 and the $1^+(E1)2^-(E2/M1)2^-$ cascade with a maximum A_2 of 0.22, thereby fixing the spin and parity of the 335-keV level at 1^-.

The spin and parity values for the levels at 255, 425, and 432 keV are limited to 0^- or 1^- by the β feeding to these levels. The A_2 values for the cascades through the 255-keV level are within 2σ of the zero value characteristic of spin 0 intermediate levels. We show this level as 0^- or 1^- in Fig. 4. If the 255-keV level is 0^-, the 432-keV level cannot be 0^- because of the strong 177-keV transition between these two levels. In addition, if the 255-keV level is 1^-, the 432-keV level cannot be 0^- since the δ values for the 255-keV transition determined from a

949-255 keV $1^+(E1)1^-(M1/E2)2^-$

cascade is not in agreement with the δ values for a

177-255 $0^-(M1)1^-(M1/E2)2^-$

cascade. Therefore, 0^- is not possible for the spin and parity of the 432-keV level for either of the possibilities for the 255-keV level, leaving 1^- as the assignment shown

TABLE V. Q_β results for ^{142}Ba decay. All energies in keV.

Q_β	γ gate	^{142}La level	$E_{\beta\max}$
2200±25	425	425	1775±35
	1001	1078	1103±30
	+ 1078		
	840		
	+ 895	1204	1011±30
	+ 949		
	+ 1204		

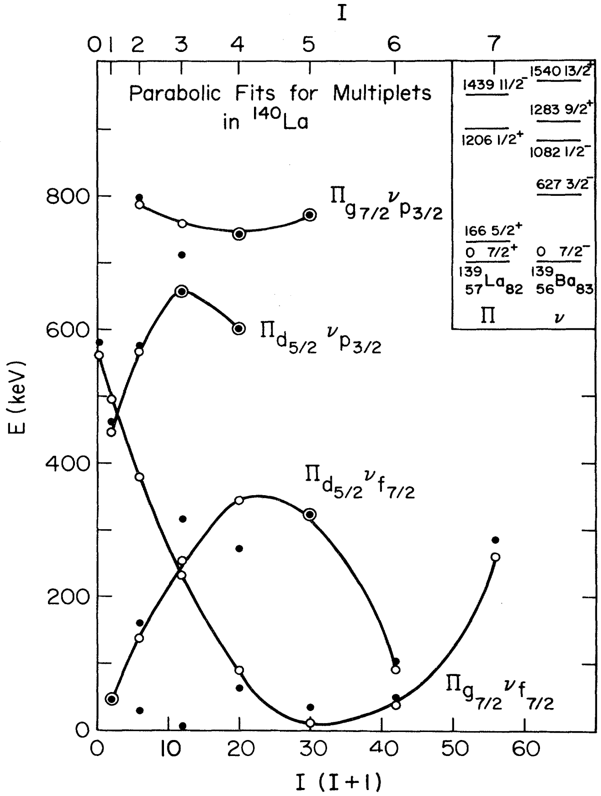

FIG. 5. The low lying levels of ^{140}La along with the levels of ^{139}La and ^{139}Ba and the parabolic fits for the proton-neutron multiplets in ^{140}La. The open circles are the fitted points and the closed circles are the experimental points. The level schemes are taken from Refs. 29, 30, and 31.

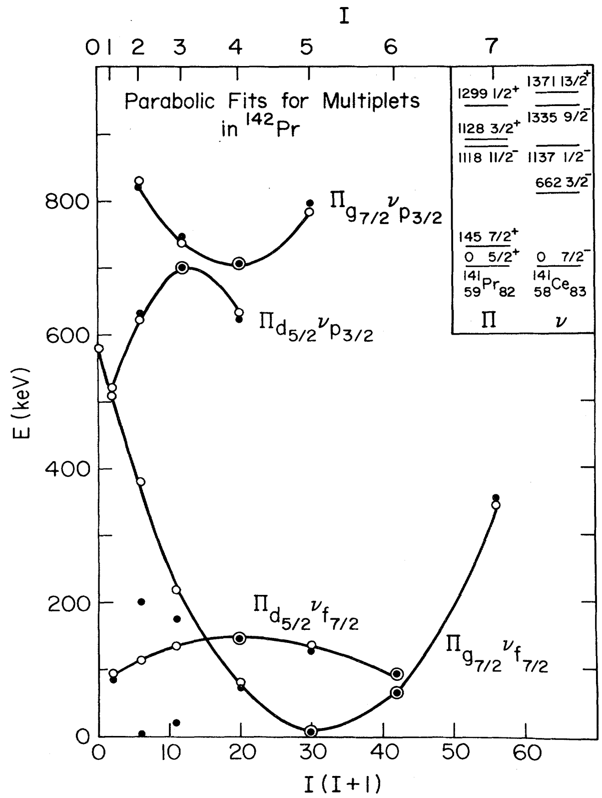

FIG. 6. The low lying levels of ^{142}Pr along with the levels of ^{141}Pr and ^{141}Ce and the parabolic fits for the proton-neutron multiplets in ^{142}Pr. The open circles are the fitted points and the closed circles are the experimental points. The level schemes are taken from Refs. 29, 32, and 33. Some of the spin and/or parity assignments have been estimated by us and are consistent with the properties of the levels.

in Fig. 4. The nonzero anisotropy for the cascade through the 425-keV level indicates a 1^- assignment for this level.

The levels at 145, 231, 300, and 361 keV are not fed by β decay nor by γ decay of any of the 1^+ levels above 1050 keV, and are candidates for spins greater than 2. The levels at 77 and 417 keV are fed by several of the 1^+ levels above 1050 keV and are limited to 0^-, 1^-, or 2^- spin and parity. Since the isomeric 145-keV level feeds the 77-keV level by the 68-keV $E2$ γ ray transition and not the 2^- ground state, the spin of the 77-keV level must be at least 2 and the 145-keV level must be ≥ 4 to avoid leaving an $M1$ path open between the 145-keV level and the 2^- ground state. We have given tentative 2^- and 4^- assignments to the 77- and 145-keV levels, respectively, and tentative 3^- assignments to the 231-, 300-, and 361-keV levels. These assignments are all consistent with the γ-ray branching into and out of these levels from and to levels with established spins and parities.

The 147-keV level is constrained to 0^-, 1^-, or 2^- by a weak β branch and a weak, tentatively placed 931-keV γ ray from the 1^+ level at 1078 keV.

The levels lying at 666, 866, 969, 984, and 1010 keV are not fed by β decay and are observed because of their feeding from the 1^+ levels above 1050 keV. They are thus limited to $0^{\pm}$, $1^{\pm}$, $2^{\pm}$, and 3^+ spins and parities. The decay of the 984-keV level to levels tentatively assigned 2^- and 3^- suggest a 2^+ assignment for this level.

VI. PARABOLIC ENERGY DEPENDENCE OF THE MULTIPLETS IN $^{140}_{57}La_{83}$ AND $^{142}_{59}Pr_{83}$

In a recent paper, we[11] showed the quantitative parabolic relationship between the members of a number of multiplets in odd-odd $N=83$ nuclides and $I(I+1)$ using a method outlined by Paar[9] and Arvay et al.[10] In this section we will extend the results of that analysis to higher-lying multiplets in ^{140}La and ^{142}Pr and use these results in the next section to project the splitting of the low-lying multiplets in ^{142}La.

In Fig. 5 are shown the low-lying levels of $^{140}_{57}La_{83}$ which has a single neutron beyond the closed shell at $N=82$ and lies at the midpoint of the $Z=50$ to 64 proton subshell. In Fig. 6 are shown the low-lying levels of $^{142}_{59}Pr_{83}$. The parabolic fits for four low-lying multiplets and the single particle levels of the adjacent odd-mass nuclides are shown in both figures.

The parabolic fits to the equation

$$E(I)=A'[I(I+1)-I_\nu'(I_\nu'+1)]^2 \quad (1)$$

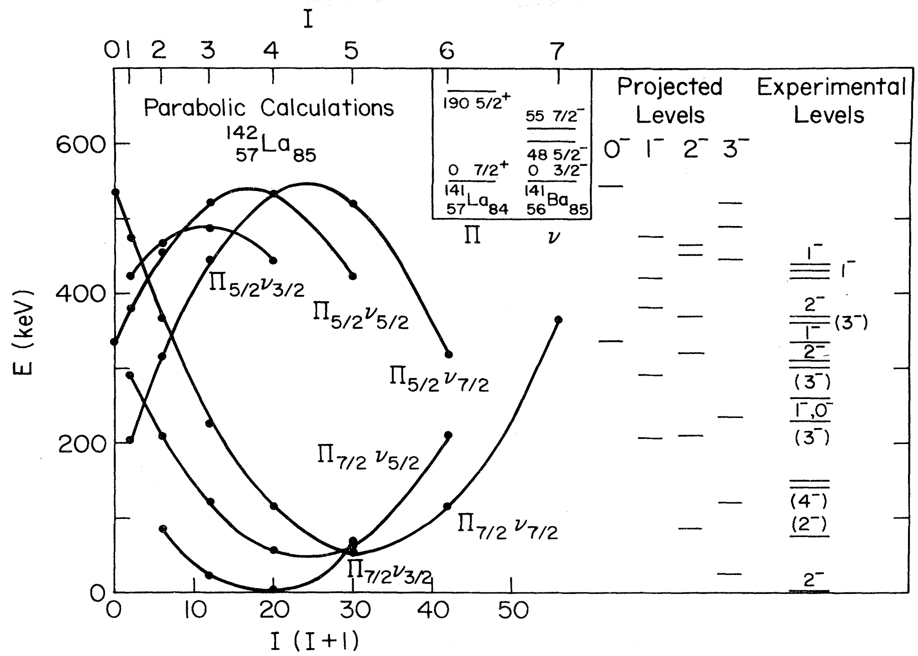

FIG. 7. The low lying levels of ^{142}La along with the levels of ^{141}La and ^{141}Ba and the parabolic fits for the proton-neutron multiplets in ^{142}La. The calculated parabolas are to the left and the low spin level scheme projected from the parabolas are shown under the heading of projected levels. The level schemes for the odd-mass nuclides are taken from Refs. 29 and 35.

are shown for the $\pi_{g_{7/2}}\nu_{f_{7/2}}$, $\pi_{d_{5/2}}\nu_{f_{7/2}}$, $\pi_{g_{7/2}}\nu_{p_{3/2}}$, and $\pi_{d_{5/2}}\nu_{p_{3/2}}$ multiplets where A' is related to the quadrupole and dipole interaction strength and $I'_\upsilon(I'_\upsilon+1)$ is given by

$$I'_\upsilon(I'_\upsilon+1)=[J_p(J_p+1)+J_n(J_n+1)-\tfrac{1}{2}]$$
$$-2\frac{\alpha_1}{\alpha_2}J_pJ_n\mathscr{V}\xi\ , \qquad (2)$$

where J_p is the proton orbital, J_n the neutron orbital, α_1 the spin vibration strength, α_2 the quadrupole vibration strength, $\mathscr{V}$ is an occupation number with a value of $+1$ if both the proton and neutron are particles or holes and -1 if one is a particle and one a hole, and ξ is a parameter dependent on the Nordheim number with absolute values ranging from 1 to 3.

The energy of a proton neutron multiplet arising from the quadrupole interaction is given by

$$\Delta E_2=\frac{-\alpha_2\mathscr{V}[I(I+1)-J_n(J_n+1)-J_p(J_p+1)]^2+[I(I+1)-J_n(J_n+1)-J_p(J_p+1)]}{2J_n(2J_n+2)2J_p(2J_p+2)}+\frac{\alpha_2\mathscr{V}}{12}\ . \qquad (3)$$

The first term gives the splitting of the multiplet and the second term gives the displacement of the whole multiplet. Because of the negative sign of the first term, a positive $\mathscr{V}$ means the levels with spins distant from the vertex will be the lowest in energy and the multiplet will be concave downward. Since the $\alpha_2\mathscr{V}/12$ has a positive sign, the whole multiplet will be shifted upward in energy. A negative $\mathscr{V}$ has the opposite effect, giving a parabola that opens upward with the whole multiplet shifted down in energy. α_2 is an effective quadrupole interaction parameter that is a product of a quadrupole interaction parameter $\alpha_2^{(0)}$ and terms correcting the interaction for quasiparticle blocking,

$$\alpha_2=\alpha_2^{(0)}\,|\,(U_{J_p}^2-V_{J_p}^2)(U_{J_n}^2-V_{J_n}^2)\,|\ . \qquad (4)$$

$\alpha_2^{(0)}$ is directly related to $B(E2)$ for the 2^+ to 0^+ transition in the adjacent even-even core by

$$\alpha_2^{(0)}=\frac{20}{3}\frac{\pi}{\hbar\omega_2}\frac{1}{Z^2R^4}\langle k\rangle^2B(E2)_{\rm vib}\ , \qquad (5)$$

where $\langle k\rangle$ is $\approx$40 MeV and $\hbar\omega_2$ is the energy of the adjacent quadrupole phonon.[34]

Where no contributions from the spin-vibration phonon are considered, the parabola can be fit by the equation

$$E(I)=A[I(I+1)-I_\upsilon(I_\upsilon+1)]^2\ , \qquad (6)$$

where

$$I_\upsilon(I_\upsilon+1)=J_n(J_n+1)+J_p(J_p+1)-\tfrac{1}{2} \qquad (7)$$

and

$$A=\frac{\alpha_2\mathscr{V}}{2J_p(2J_p+2)2J_n(2J_n+2)}\ . \qquad (8)$$

The contribution to the energy from the spin-vibration phonon is linear in $I(I+1)$ and is also given by an equation with two terms with opposite signs, one of which is a constant:

TABLE VI. Parabolic fits to the multiplets in odd-odd $N=83$ isotones.

Nuclide	Multiplet	Levels fit (σ in keV)	A' (eV)	$I'_v(I'_v+1)$	$I_v(I_v+1)$	α_2 (MeV)	α_1 (MeV)	$\alpha_2\mathscr{V}/12$ (keV)	E_v (keV)[a] Calc.	E_v (keV)[a] Fit	$B(E2)$[b]	U_p^2	V_p^2[c]
$^{140}_{57}La_{83}$	$\pi g_{7/2}\times\nu f_{7/2}$	5(20)	505	33.4	31	2.23	0.17	−186	0	0	0.22	0.37	0.63
	$\pi d_{5/2}\times\nu f_{7/2}$	4(33)	−692	22.8	24	1.26	0.05	105	457	327		0.58	0.42
	$\pi g_{7/2}\times\nu p_{3/2}$	3(5)	270	20	19	0.25	0.01	−21	792	744		0.49	0.51
	$\pi d_{5/2}\times\nu p_{3/2}$	4(4)	−1487	13.7	12	0.89	0.09	74	1053	658		0.56	0.44
$^{142}_{59}Pr_{83}$	$\pi g_{7/2}\times\nu f_{7/2}$	4(5)	584	31.5	31	2.27	0.04	−189	0	0	0.29	0.38	0.62
	$\pi d_{5/2}\times\nu f_{7/2}$	4(6)	−146	21.1	24	0.27	0.02	22	66	144		0.52	0.48
	$\pi g_{7/2}\times\nu p_{3/2}$	4(6)	704	19.4	19	0.56	0.01	−47	804	705		0.48	0.52
	$\pi d_{5/2}\times\nu p_{3/2}$	3(2)	−1454	13.2	12	0.55	0.05	46	752	702		0.53	0.47

[a] E_v (calculated) is given by $E_{J_n}+E_{J_p}+\alpha_2\mathscr{V}/12$, where E_{J_n} and E_{J_p} are the experimentally observed positions of the single particle levels in the adjacent odd-mass nuclide. E_v (fit) is the position of the vertex in the fit. The results are normalized to the observed ground state.

[b] Weighted average of experimental data for the $B(E2)$ value of the adjacent even-even core taken from Refs. 31 and 36 in units of $10^{-48}\,e^2\,\text{cm}^4$.

[c] V_n^2, the probability of the single neutron occupation in the $f_{7/2}$ state, is assumed to be 0.125.

$$\Delta E_1=\frac{-\alpha_1\xi I(I+1)}{(2J_n+2)(2J_p+2)}+\alpha_1\xi\frac{[J_n(J_n+1)+J_p(J_p+1)]}{(2J_n+2)(2J_p+2)}\ . \qquad (9)$$

Here

$$\alpha_1=4\alpha_1^{(0)}U_{J_p}V_{J_p}U_{J_n}V_{J_n}\ . \qquad (10)$$

$\alpha_1^{(0)}$ is the spin vibration interaction defined by Paar.[9] The inclusion of the spin-vibration term adds the second term to the formula for $I'_v(I'_v+1)$ that is shown in Eq. (2).

In Table VI we show the fitting parameters for the eight multiplets identified in ^{140}La and ^{142}Pr, along with the α_1, α_2, and multiplet displacement values deduced from them. The difference between $I'_v(I'_v+1)$ and $I_v(I_v+1)$ is used to determine α_1/α_2, which is then used to extract α_2 from A'. The quenching of the df multiplet in ^{142}Pr as a result of the increased occupancy is clearly demonstrated as A falls from −693 eV to −146 eV while V_p^2 arises from 0.42 to 0.48, and $(U_p^2-V_p^2)$ falls from 0.16 to 0.04.

The displacements of the vertices of the multiplets are calculated from the $\alpha_2\mathscr{V}/12$ terms listed in Table VI. The separation between the df and gf multiplets in ^{140}La is thus calculated by adding the $\alpha_2\mathscr{V}/12$ terms for each multiplet to the 166-keV difference between the $\frac{7}{2}^+$ and $\frac{5}{2}^+$ states in ^{139}La. As is seen in Table VI the calculated values average within ~80 keV of the observed values except for the dp multiplet in ^{140}La.

Significant departures from the parabolas are noted for the 2^- and 3^- levels. These departures give rise to the 3^- ground state in ^{140}La and the 2^- ground state of ^{142}Pr, both of which violate the Nordheim[1] or Brennan-Bernstein[3] "rules" for odd-odd nuclei. Since the 3^- levels lie near the intersection of the gf and df parabolas, their repulsion is not unexpected. Overall, the α_1 values appear to play only a small role in the multiplet splitting observed.

VII. PROJECTED LOW-LYING MULTIPLETS IN ^{142}La

The general success[11] of the parabolic fits for the splitting and displacement of the low-lying $N=83$ multiplets makes it possible to project the low-lying level structure for ^{142}La from the specific parameters observed for ^{140}La and ^{142}Pr and the structure of the adjacent odd-mass ^{141}La and ^{141}Ba nuclides. First, we note the small role of α_1 and set $\alpha_1\equiv 0$, and use Eq. (6) for these projections. The parameters required to compute the multiplet splitting are A and $I_v(I_v+1)$ while the displacement of whole multiplets requires $\alpha_2\mathscr{V}/12$ values. As can be seen in Eqs. (8), (4), and (5), A is proportional to $(U_{J_p}^2-V_{J_p}^2)$, $(U_{J_n}^2-V_{J_n}^2)$, and $B(E2)$ and inversely proportional to $\hbar\omega_2$, the energy of the adjacent quadrupole phonon. The first 2^+ level in ^{140}Ba is $\sim\frac{1}{2}$ the energy of the 2^+ level in ^{138}Ba and the $B(E2)$ value for ^{140}Ba can be estimated[37] to be between 1.5 and 2.0 times larger than the $B(E2)$ value in ^{138}Ba. The low-lying triplet observed in ^{141}Ba is assumed to be primarily a $(f_{7/2})^3\ \frac{3}{2},\frac{5}{2},\frac{7}{2}$ cluster that has been described by Paar *et al.*[38] Thus, all three levels need the same $(U_{J_n}^2-V_{J_n}^2)$ term for $f_{7/2}$ orbitals as indicated by Arvay *et al.*[10] Consequently, since there are now three $f_{7/2}$ neutrons in ^{142}La, the neutron occupancy factor $(U_{J_n}^2 - V_{J_n}^2)$ will be smaller by a factor of three. We have elected to assume that the increased $B(E2)$ and $1/\hbar\omega_2$ compensate the decreased $(U_{J_n}^2 - V_{J_n}^2)$ term and have used $A_{gf} = 0.50$ keV and $A_{df} = -0.70$ in Eq. (6) to calculate the six parabolas shown in Fig. 7. The multiplet displacement terms have also been computed using the same $\alpha_2\mathscr{V}/12$ terms found in ^{140}La.

The comparison of the calculated and experimental levels reveals several important features. First, the calculated level density is close to the observed level density. Thirteen low-lying 0^-, 1^-, and 2^- states that can be fed by β decay plus up to three low-lying 3^- states that can be γ fed would be expected. These can be compared with thirteen observed low-lying 0^-, 1^-, 2^-, and 3^- states and one 4^- state.

Second, the 4^- isomer is likely to be the bottom of one of the three $\mathscr{V} = -1$ parabolas whereas the 2^- ground and first excited levels are probably depressed in the same manner as the 2^- levels in ^{140}La. As the calculated half-life of 1 μs for a 68-keV $E2$ single particle transition is quite close to the observed 0.87 μs half-life, the decay of the isomer can be viewed as a single particle transition from one multiplet to another.

The absence of any 145-keV $E2$ crossover transition from the 145-keV isomer to the 2^- ground state requires an $E2$ retardation of ≥ 50. As large as that is, it is matched by the retardation of the unobserved 177-keV transition between the 0^- or 1^- 255-keV level and the 2^- level at 77 keV. Since an upper limit of ≈ 3 can be set for the intensity of such a transition it must be hindered by a factor of 100 if it is $M1$, or a factor of 50 if it is $E2$. Thus, it may be postulated that the ground state 2^- level differs from the 4^- isomer in both its neutron and proton configuration. There are a number of other weak or unobserved transitions between levels where $M1$ multipolarity is possible whose hindrance may be a consequence of different proton and neutron configurations of the initial and final states. No attempt has been made, however, to try to identify any of the observed levels with a particular configuration.

We conclude that the parabolic relationships that worked well for the $N = 83$ nuclides are also useful to describe multiplet splitting and displacements as well as transition hindrances for the odd-odd $N = 85$ nuclide ^{142}La. It is interesting to note that the six parabolas will invert in ^{144}La as the next pair of neutrons will lift the occupancy of the $f_{7/2}$ orbitals over 0.5. Then the gf parabolas will open down and the df parabolas will open up. The 3^- ground state and 4^- first excited state could be the bottom of the $\pi_{5/2}\,\nu_{5/2}$ parabola.[39] Unfortunately, the structure of the adjacent ^{143}Ba and ^{143}La odd mass nuclides is not well enough established[40] for a more detailed comparison.

ACKNOWLEDGMENTS

The authors wish to express their appreciation to the U.S. Department of Energy for the support of this work. The efforts of the technical staff during the collection and analysis of these data are gratefully acknowledged. The helpful discussions with Dr. R. F. Casten have been of much value. The hospitality of the Physics Department and Neutron-Nuclear Physics Group for the non-BNL authors has been much appreciated. One of us (W.B.W.) wishes to acknowledge the support of the University of Maryland Graduate School through a Semester Research Award.

*Present address: Institute of Nuclear Science, National Tsing Hua University, Taiwan, Republic of China.
†Present address: 11 Pinsker St., Rehovot, Israel.
‡Present address: Physics Dept., Nuclear Research Center Negev, Box 9001, Beer Sheba, 84190 Israel.

[1]L. W. Nordheim, Rev. Mod. Phys. 23, 322 (1951).
[2]C. J. Gallagher, Jr., and S. A. Moszkowski, Phys. Rev. 111, 1282 (1958).
[3]M. H. Brennan and A. M. Bernstein, Phys. Rev. 120, 927 (1960).
[4]A. DeShalit, Phys. Rev. 91, 1479 (1953).
[5]K. Sasaki, Nucl. Phys. 71, 95 (1965).
[6]J. P. Schiffer, Ann. Phys. (N.Y.) 66, 798 (1971).
[7]A. Molinari, M. B. Johnson, H. A. Bethe, and W. M. Alberico, Nucl. Phys. A239, 45 (1975).
[8]H. C. Chiang, M. C. Wang, and S. T. Hseih, Lett. Nuovo Cimento 34, 370 (1982).
[9]V. Paar, Nucl. Phys. A331, 16 (1979).
[10]Z. Arvay, T. Fenyes, J. Gulyas, T. Kibedi, E. Koltay, A. Krasznahorkay, S. Laszlo, P. Novak, S. Brant, and V. Paar, Phys. Scr. 26, 57 (1982).
[11]W. B. Walters, C. Chung, D. S. Brenner, A. Aprahamian, R. L. Gill, R. E. Chrien, A. Wolf, M. Shmid, and L.-J. Yuan, Phys. Lett. B (in press).
[12]O. Hahn and F. Strassmann, Naturwissenschaften 27, 11 (1939).
[13]L. P. McIsaac and E. L. Murri, Nucl. Phys. A156, 212 (1970).
[14]J. T. Larsen, W. L. Talbert, Jr., and J. R. McConnell, Phys. Rev. C 3, 1372 (1971).
[15]K. Fritze and T. J. Kennett, Phys. Rev. 127, 1262 (1962).
[16]R. L. Gill, M. L. Stelts, R. E. Chrien, V. Manzella, H.-I. Liou, and S. Shostak, Nucl. Instrum. Methods 186, 243 (1981).
[17]M. Shmid, R. L. Gill, and C. Chung, Nucl. Instrum. Methods (in press).
[18]A. Wolf, C. Chung, W. B. Walters, R. L. Gill, M. Shmid, H.-I. Liou, M. Stelts, R. Chrien, G. Peaslee, and D. S. Brenner, Nucl. Instrum. Methods 206, 397 (1983).
[19]W. L. Talbert, Jr., F. K. Wohn, L. J. Alquist, and C. L. Duke, Phys. Rev. C 23, 1726 (1981).
[20]D. M. Rehfield, Nucl. Instrum. Methods 157, 351 (1978).
[21]H. G. Borner, W. F. Davidson, J. Almeida, J. Blachot, J. A. Pinston, and P. H. M. VanAssche, Nucl. Instrum. Methods 164, 579 (1979).
[22]D. C. Camp and A. L. Van Lehn, Nucl. Instrum. Methods 76, 192 (1969).
[23]H. W. Taylor, B. Singh, F. S. Prato, and R. McPherson, Nucl. Data Tables 9, 1 (1971).
[24]A. J. Becker and R. M. Steffen, Phys. Rev. 180, 1043 (1969).
[25]F. Rosel, H. M. Fries, K. Alder, and H. C. Pauli, Atomic Data Nucl. Data Tables 21, 236 (1978).
[26]W. V. Prestwich and T. J. Kennett, Phys. Rev. 134, B485 (1964).

[27]S. Raman and H. B. Gove, Phys. Rev. C 7, 1995 (1973).
[28]H. O. Denschlag, Institute von Lave Langevin (ILL) annual report 1981 (unpublished), p. 25.
[29]*Table of Isotopes,* edited by C. M. Lederer and V. Shirley, (Wiley, New York, 1977).
[30]L. K. Peker, Nucl. Data Sheets 32, 1 (1981).
[31]L. K. Peker, Nucl. Data Sheets 28, 267 (1979).
[32]J. K. Tuli, Nucl. Data Sheets 23, 529 (1978).
[33]J. K. Tuli, Nucl. Data Sheets 25, 53 (1978).
[34]A. Bohr and B. Mottelson, *Nuclear Structure* (Benjamin, New York, 1975), Vol. 2.
[35]H. Yamamoto, F. K. Wohn, K. Sistemich, A. Wolf, W. B. Walters, C. Chung, R. L. Gill, M. Shmid, R. E. Chrien, and D. S. Brenner, Phys. Rev. C 26, 1215 (1982).
[36]S. C. Pancholi and M. J. Martin, Nucl. Data Sheets 18, 167 (1976).
[37]S. M. Scott, D. D. Warner, W. D. Hamilton, P. Hungerford, G. Jung, K. D. Wunsch, and B. Pfeiffer, J. Phys. G 5, 487 (1979).
[38]V. Paar, G. Vanden Berghe, C. Garrett, J. R. Leigh, and G. D. Dracoulis, Nucl. Phys. A350, 139 (1980).
[39]C. Chung, W. B. Walters, R. L. Gill, M. Shmid, R. E. Chrien, and D. S. Brenner, Phys. Rev. C 26, 1198 (1982).
[40]J. K. Tuli, Nucl. Data Sheets 25, 603 (1978).